

The Influences of Complexing agents on Growth of Zinc Oxide Thin Films from Zinc Acetate Bath and Associated Kinetic Parameters

A. I. Inamdar, S. H. Mujawar, P. S. Patil*

Thin Film Materials Laboratory, Department of Physics, Shivaji University, Kolhapur-416 004, India

*E-mail: psp_phy@unishivaji.ac.in

Received: 14 July 2007 / Accepted: 18 August 2007 / Published: 1 October 2007

Zinc oxide thin films were electrodeposited from an aqueous 50 mM zinc acetate bath at room temperature on FTO coated conducting glass substrates. The effect of various complexing agents like Ethylene Diamine Tetra Acetic Acid (EDTA) and citric acid on their structural, morphological, optical and nucleation growth mechanism were studied. Zinc oxide film formation was confirmed by using X-ray diffractometer. The band gap of the films deposited using different complexing agents is in the range of 3.25 to 3.3 eV. Zinc oxide thin films show different morphologies like cauliflower, granular and compact structure when depositions were carried out in absence and presence of complexing agents. According to Scharifker and Hills nucleation growth mechanism films deposited without complexing agents and those deposited with EDTA follows 3D instantaneous nucleation and growth mechanism while films in presence of citric acid arrested type of growth is observed due to influence of citric acid molecules over studied time domain. The effect of complexing agents on nuclei density (N_0), saturated nuclei density (N_{sat}) and nucleation rate constant (A) were studied and found that the values of these kinetic parameters decrease in presence of complexing agents.

Keywords: Zinc oxide thin films, Electrodeposition, X-ray diffractometer, Scanning Electron Microscopy (SEM), Spectrophotometer,

1. INTRODUCTION

ZnO is attracting considerable attention for its possible application to UV light emitters, spin functional devices, gas sensors, transparent electronics and surface acoustic wave devices. There is also interest in integrating ZnO with other wide band gap ceramic semiconductors such as the AlInGaN system. It has advantages relative to GaN because of its availability in bulk, single-crystal form and its larger exciton binding energy (60 meV, .25 meV for GaN) [1]. ZnO is a direct wide band gap (~3.3 eV) material with a large exciton binding energy of 60 meV. This makes it interesting as a

laser material based on exciton recombination at room temperature or even higher [2]. ZnO is a candidate host for solid state blue to UV optoelectronics, including laser development. This has important applications in high density data storage systems, solid-state lighting (where white light is obtained from phosphors excited by blue or UV light-emitting diodes), secure communications and bio-detection [3].

ZnO has received much attention over the past few years because it has a wide range of properties that depend on doping, including a range of conductivity from metallic to insulating (including *n*-type and *p*-type conductivity), high transparency, piezoelectricity, wide-band gap semiconductivity, room-temperature ferromagnetism, and huge magneto-optic and chemical-sensing effects [2]. ZnO has an extensive range of functional properties important to applications in optoelectronics, spintronics, and piezoelectric transducers [4]. Recently there has been much interest in the electronic and photonic properties of ZnO nanostructures as foreseeable applications include photo cells and laser diodes [5]. The synthesis of 1D single-crystalline ZnO nanostructures has been of growing interest owing to their promising application in nanoscale optoelectronic devices. Single-crystalline ZnO nanowires have been synthesized successfully in several groups [6]. Ordered porous ZnO films are useful for the application in sensors and semi conducting electrodes [7].

In the recent years the control over the properties of ZnO through chemical route has attracted increasing interest, and many methods for the deposition of ZnO thin films were reported. Among all these methods, pulsed laser deposition [8], spray pyrolysis [9], sputtering [10], sol-gel [11], electrochemical deposition has shown powerful ability to control the crystallization engineering of ZnO [12]. The effect of capping agent like citric acid on morphology of zinc oxide deposit was studied by C. Xie [13]. The effect of complexing agent on nucleation and growth mechanism has been sparsely studied.

In the present work we report the effect of complexing agents on the nucleation and growth mechanism of zinc oxide thin films. The study on the nucleation density (N_0), saturated nuclei density (N_{sat}) and nucleation rate constant (A) is presented with the view to understand the effect of complexing agents.

2. EXPERIMENTAL PART

Zinc oxide electrodeposition was carried out in an aqueous solution containing 50 mM of zinc acetate solution (Thomas Baker, 99.5%) and 0.1M KCl introduced to increase the conductivity of an electrolyte. Initially pH of as-prepared zinc acetate solution was 6. The bath was maintained at 10.5 by using 0.5 M KOH solution to deposit ZnO thin films, in consultation with Pourbaix diagram. To avoid precipitation of the bath, Ethylene Diamine Tetra acetic Acid (EDTA) and citric acid are used as complexing agents. Ex-situ oxygen was bubbled through all the baths.

A three electrode electrochemical cell was used for electrochemical studies and film deposition. FTO substrate of 3 cm² area is used as a working electrode, a helical platinum wire as a counter electrode and saturated calomel electrode (SCE) as a reference electrode (SCE $E_0 = 0.244$ V Vs SHE, the saturated hydrogen electrode). The electrodes were placed parallel to each other separated by a

distance of 2 cm. Thin films of zinc oxide were obtained by potentiostatic electrolysis at -0.750 V (Vs SCE) for 30 minutes in a zinc acetate bath. The films prepared by using different complexing agents viz EDTA and citric acid are denoted by B and C respectively. Those deposited without using complexing agent are denoted by A.

Cyclic voltammetry (CV) and chronoamperometric (CA) studies were carried out using scanning potentiostat EG & G versastat-II model PAR-362. The surface morphology of samples was observed using the JEOL-JSM 6360 scanning electron microscope (SEM). X-ray diffraction (XRD) spectra of the films were recorded on an X-ray diffractometer (Philips PW-3710) with Cu-K α radiation of 1.5418\AA wavelength. The optical transmittance and absorption were measured by using Systronic make UV-VIS 119 spectrophotometer.

3. RESULTS AND DISCUSSION

Figure 1 shows the XRD patterns of the films prepared from 50 mM aqueous zinc acetate solution concentration at depositions potential -0.750 V (Vs SCE) on to FTO coated conducting glass substrates. The observed d values compared with standard d values and are in good agreement with standard d values. The films prepared in absence of complexing agent at pH 6 (figure 1 A) shows reflections along (002) (200) and (203) planes corresponding to formation of hexagonal wurtzite structure of zinc oxide, in addition to these peaks along (101) and (112) correspond to metallic zinc formation. The films deposited without complexing agent were grayish black with luster. It is therefore

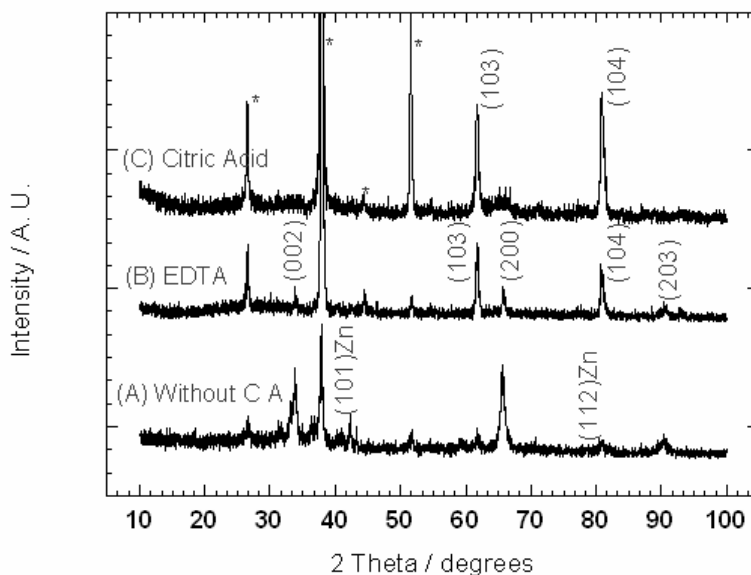


Figure 1. XRD spectra of the Zinc oxide thin films deposited via 50 mM aqueous Zinc acetate solution using different complexing agents.

apparent that the deposition of metallic Zn is an unwanted reaction to the desired ZnO formation. Therefore further experiments were performed at pH 10.5 using different complexing agents (EDTA and citric acid) to complex the Zn^{+2} atom and to achieve the desired pH. Figure 1 (B and C) shows

XRD spectra of films deposited using EDTA and citric acid respectively. These films are transparent to the visible light. The observed 'd' values of the films were compared with JCPDS data (file number 75-1533, 36-1451) and are in good agreement with the standard 'd' values. Both the samples shows reflections along (103), (104), are the reflections of hexagonal wurtzite structure of ZnO of lattice constant $a=3.351\text{\AA}$ and $c=5.226\text{\AA}$, except these, the reflections along (002), (200) and (203) are observed for the films deposited using EDTA. All remaining peaks due to the substrate (FTO coated conducting glass) are indicated by star (*).

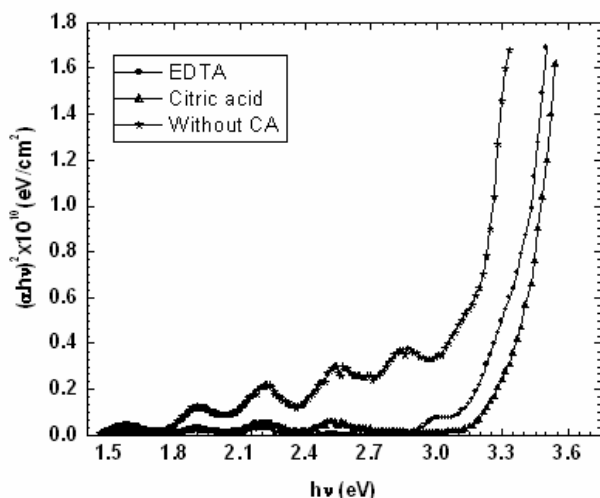


Figure 2. The plot of $(\alpha h\nu)^2$ vs $h\nu$ for the samples deposited using different complexing agents on to the FTO coated conducting glass substrates

The transmittance spectra for the films deposited using different complexing agents was recorded in the wavelength range of 350-850nm (not shown). Figure 2 shows the plot of $(\alpha h\nu)^2$ vs $h\nu$ of films prepared with and without complexing agents which is calculated from transmittance and film thickness. The transmittance for both the samples B and C is about 60% in the visible region. According to transmittance spectrum, the absorption coefficient α of the film was estimated by the expression,

$$T = e^{-\alpha d} \text{----- (1)}$$

where T is the transmittance and d is the film thickness of the films. The relation between the absorption coefficient and the incident energy $h\nu$ is expressed as [14],

$$(\alpha h\nu)^2 = A(h\nu - E_g) \text{----- (2)}$$

where A is the constant and E_g is the direct band edge. The extrapolating the linear portion of the curve to zero absorption coefficient of $h\nu$ axis an intercept at 3.3 and 3.35 eV has been deduced for

sample B and C respectively. These observed band gap is well agreement with the literature. The band energy for the films prepared without complexing agent is about 2.9 eV.

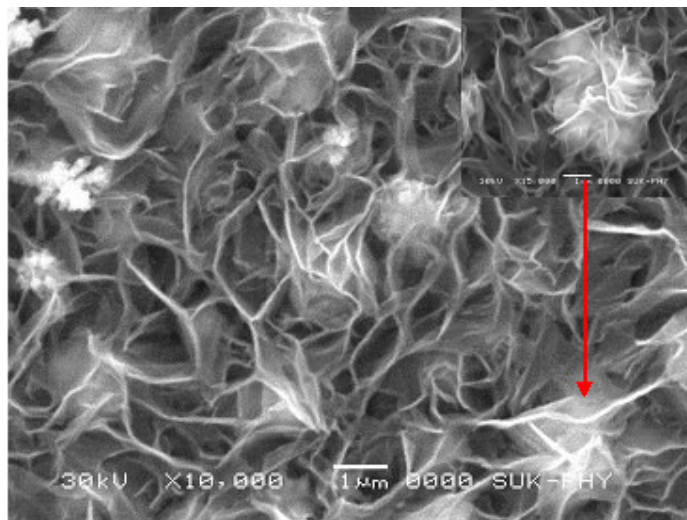


Figure 3. SEM images of solid films formed in the absence of complexing agent
Low magnified flakes and Magnified cauliflower (shown in inset)

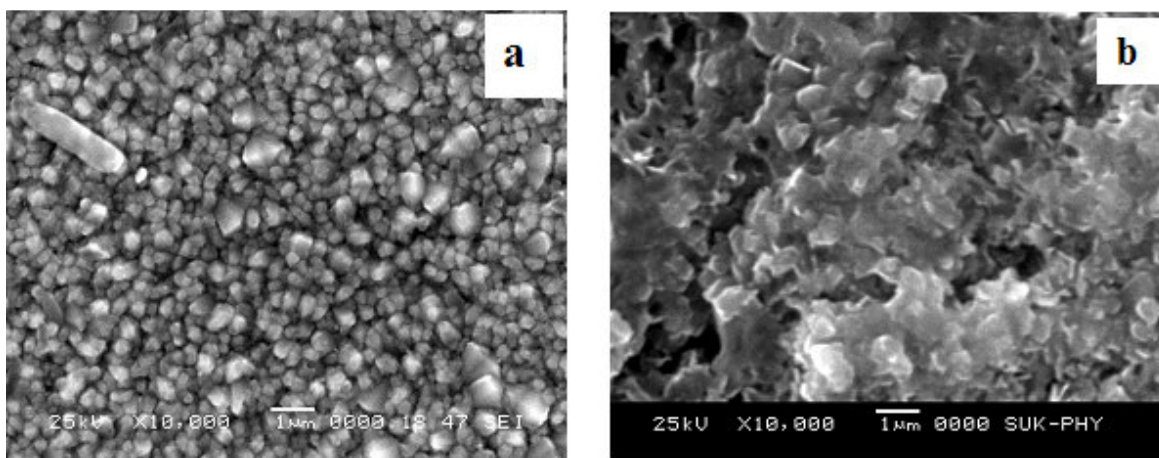


Figure 4. SEM images of solid films formed in the presence of complexing agents
(a) EDTA (b) Citric Acid

The surface morphology of the Zinc oxide layers obtained by electrodeposition has been investigated by SEM and is shown in figure 3 in absence of complexing agent and figure 4 (a and b) in presence of EDTA and citric acid respectively. Figure 3 shows a network of flakes and cauliflowers of about 1 μm diameter. Inset in figure 3 shows the magnified image of cauliflower. Figure 4 (a and b) shows the SEM images of films deposited in presence of EDTA and citric acid respectively. From figure 4 b) well defined grains of about 0.5 μm are observed in presence of EDTA as complexing

agent. Figure 4b shows SEM of sample deposited using citric acid; no well defined crystallites were observed due to restriction on precipitation. This leads to consideration that the influence of citric acid molecules is more on the crystal growth and nucleation of ZnO. Similar results were reported by H. Wang [13].

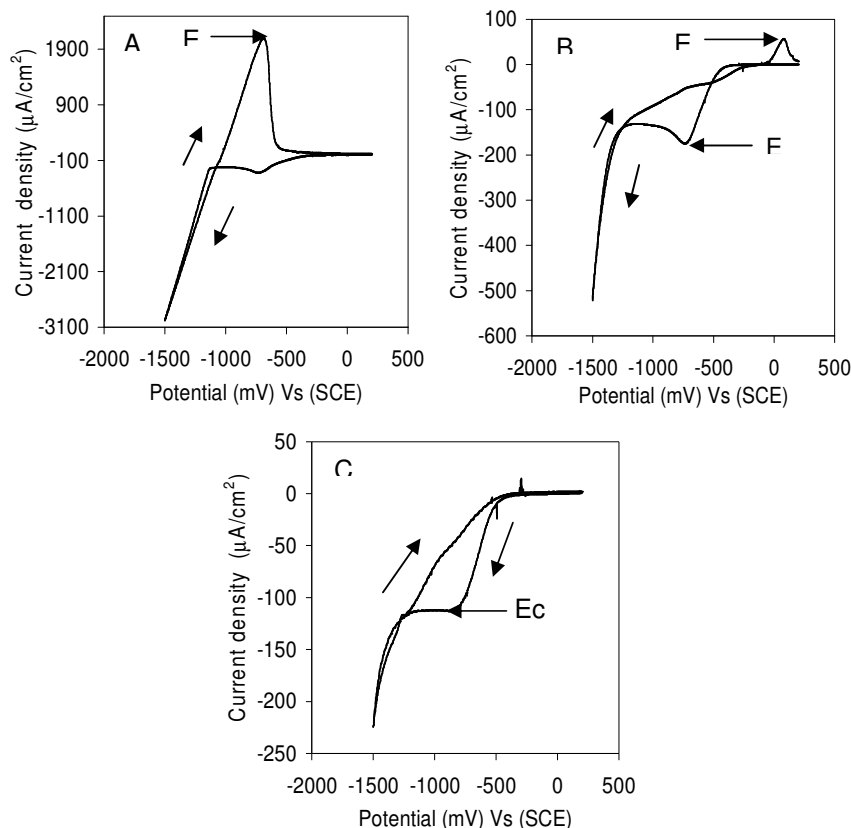


Figure 5. Shows CV spectra obtained from zinc acetate solution from pure and for the using various complexing agents.

The CV spectra (figure 5) were recorded at pH 6 and at pH 10.5 from zinc acetate solution using various complexing agents Viz. EDTA and citric acid respectively. The potential scan was started from +200 mV (SCE), reversed at -1500 mV (SCE) and terminated at +200 mV (SCE) at 20 mV/s scan rate. A well defined cathodic peak (Ec) is discernable at -706, -766 and -878 mV (vs SCE) during forward cathodic scan for the samples A, B and C respectively. During reverse scan, current decreases rapidly up to -1250 mV (vs SCE), followed by a monotonic decrement to about -400 mV (SCE). The cross-over observed in the CV spectra can be related to the onset of nucleation process [15, 16]. It is noticeable that the Zn stripping peak is observed at 0.66 V (Vs SCE) for the sample A. While Zn stripping is absent for the samples deposited using the citric acid suggesting the route to formation of metallic Zn does not occur. Similar results were reported by A. Chatterjee [17]. For the sample deposited using EDTA as a complexing agent exhibits an oxidation peak at 100 mV (vs SCE) which is much less pronounced than the reduction peak is due to the oxidation of deposited Zn at high cathode potential.

The overpotential is an important term which defines the rate of chemical reaction. The less overpotential more rapid is the chemical reaction. The values of cathodic peak potentials and overpotential ($\eta = E_{co} - E_{cp}$ where E_{co} is cross over potential) obtained from cyclic voltammograms are given in Table 1. In these cases the overpotential is required to form the first nuclei on the substrate surface and afterwards the current density quickly increases [18]. A possible reason for this behavior could be ascribed to a complexation effect of the Zn^{+2} ions by the complexing agents (EDTA and citric acid), leading to retardation in the electrodeposition kinetics. Similar results were reported by A. E. Alvarez [19]. From these it is observed that large overpotential is required to form the first nuclei on the substrate surface by using the citric acid as a complexing agent i.e the citric acid can form more complexing effect on Zn^{+2} ions than the EDTA. The values of overpotential are less for the sample deposited without complexing agents this suggests that effect of complexing agents is more on acceleration of electrochemical reaction kinetics.

Table 1. Parameters obtained from cyclic voltammetry and Chronoamperometry

Sample	Cathodic Peak Current ($\mu A/cm^2$)	Cathodic peak potential (mV)	Ci μA	Cint μA	Cf μA	Cf-Cint μA	Nucleation and Growth Mechanism
A	-304	-702	1224	1144	1492	212	Instantaneous
B	-171	-766	360	97	97	0	Instantaneous
C	-113	-878	220	110	151	41	-

Figure 6 (a, b and c) shows current versus time transients obtained from 50 mM zinc acetate bath onto FTO coated conducting glass substrates. After an initial surge, current decays abruptly as anions in the close vicinity of the electrode of the cathode are reduced and a transient signal is observed. The current C_i (shown in figure 6) depends on number of initially accessible cationic species in the close vicinity of the cathode, which discharge immediately after electrode is polarized. This leads to the birth of the nucleation centers: either large number of small nuclei or small number of large nuclei. This causes temporal depletion regime near cathode, leading to the decrement in the current; C_{int} . As fresh cationic species resume diffusing from the bulk towards electrode, current starts gradually increasing and reach C_f . Hence it is reasonable that the difference $C_f - C_{int}$ is proportional to the number of cationic species deposited onto electrode during the second step. This current is used to judge whether the nuclei formed in the first step grow progressively or instantly in second step [20].

Based on the above discussion the values of $C_f - C_{int}$ are given in the Table 1. From this it is observed that the current in case of sample A (figure 6 a) and for sample C (figure 6 c) doesn't saturate. This reveals that the growth of nuclei for the sample A and C takes place after the initial surge. Negligible rise in the current is obtained for the samples deposited using EDTA (figure 6 b) as a complexing agent i.e. the nucleation and growth takes place during the first step (initial surge).

Chronoamperometry is an electrochemical technique as it provides current time transients. Scharifker and Hills [21] used chronoamperometric technique to derive the mathematical model to describe the nucleation process: instantaneous and progressive.

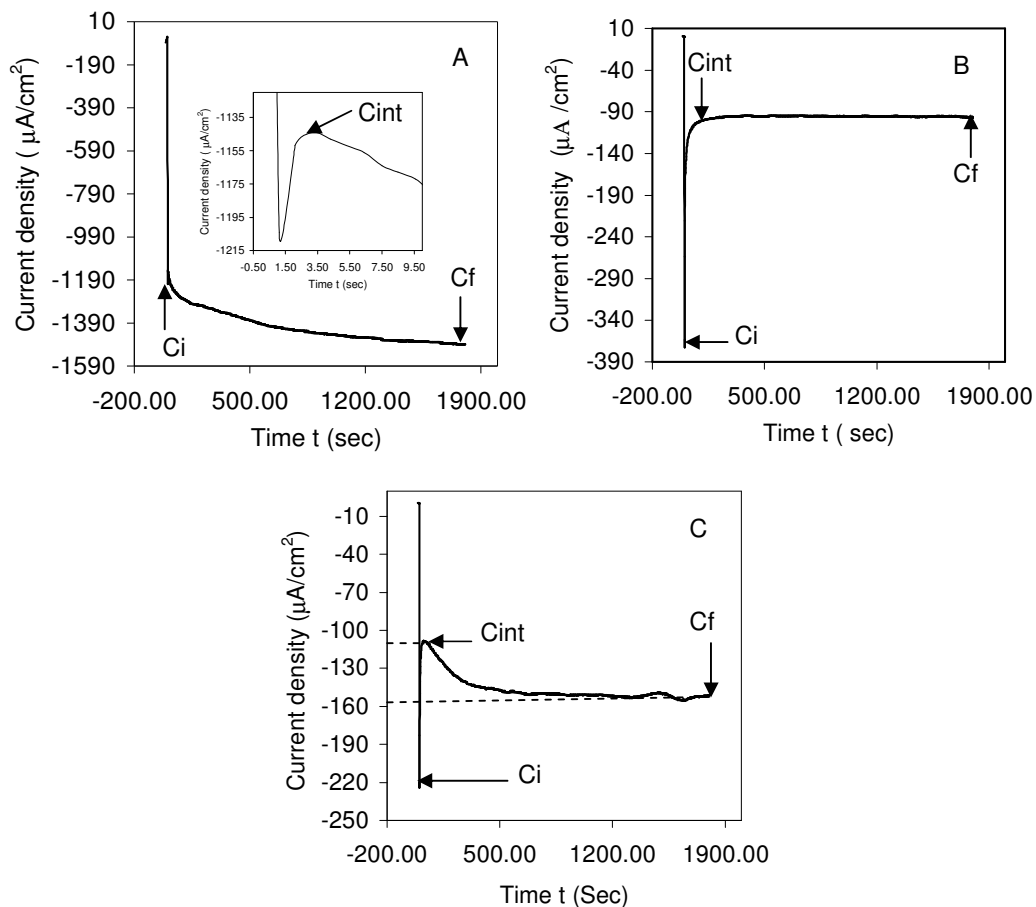


Figure 6. Shows current versus time transients obtained for pure zinc acetate solution and for using different complexing agents.

Progressive nucleation corresponds to slow growth of nuclei on a less number of active sites, all activated at same time. Instantaneous nucleation corresponds to fast growth of nuclei on many active sites, all activated during the course of electroreduction [22]. The expression for instantaneous nucleation and progressive nucleation with 3D growth (eqⁿ 2 and 3) are given in our earlier research article published in solar energy materials and solar cells [20].

According to these equations the fitting of experimental curves with theoretical curves are shown in figure 7. The experimental curves in case of sample A and B are very similar to that of instantaneous nucleation and growth mechanism in studied time domain. This suggests that the growth process in case of sample A and B is of instantaneous nature. For the samples C the experimental curve have very less current density than the current densities of theoretical curves. Films in presence of citric acid follows arrested type of growth due to a complexation effect of the Zn⁺² ions by the complexing agents (citric acid), leading to retardation in the electrodeposition kinetics.

According to the nucleation and growth the kinetic parameters nucleation density ($N_0 \text{ cm}^{-1}$), saturated nuclei density ($N_{\text{sat}} \text{ cm}^{-1}$) and nucleation rate constant (A) are derived from the following equations [21, 23, 24].

$$KN_0 = \left[\frac{0.2552zFC}{I_m t_m} \right]^2 \quad \text{(Instantaneous Nucleation) ----- (3)}$$

$$K'N_{\text{Sat}} = \left[\frac{0.4734zFC}{I_m t_m} \right]^2 \quad \text{(Progressive Nucleation) ----- (4)}$$

where $K = \left[\frac{8\pi CM}{\rho} \right]^{1/2}$ and $K' = \frac{4}{3} \left[\frac{8\pi CM}{\rho} \right]^{1/2}$

$$A = \frac{1.2141(zFC)^2}{\pi K I_m^2 t_m^3} \quad \text{(Instantaneous Nucleation) ----- (5)}$$

where z is the number of equivalent, C is the concentration of active cation, M is the molecular weight, ρ is the density of deposit and F is the Faradays rate constant.

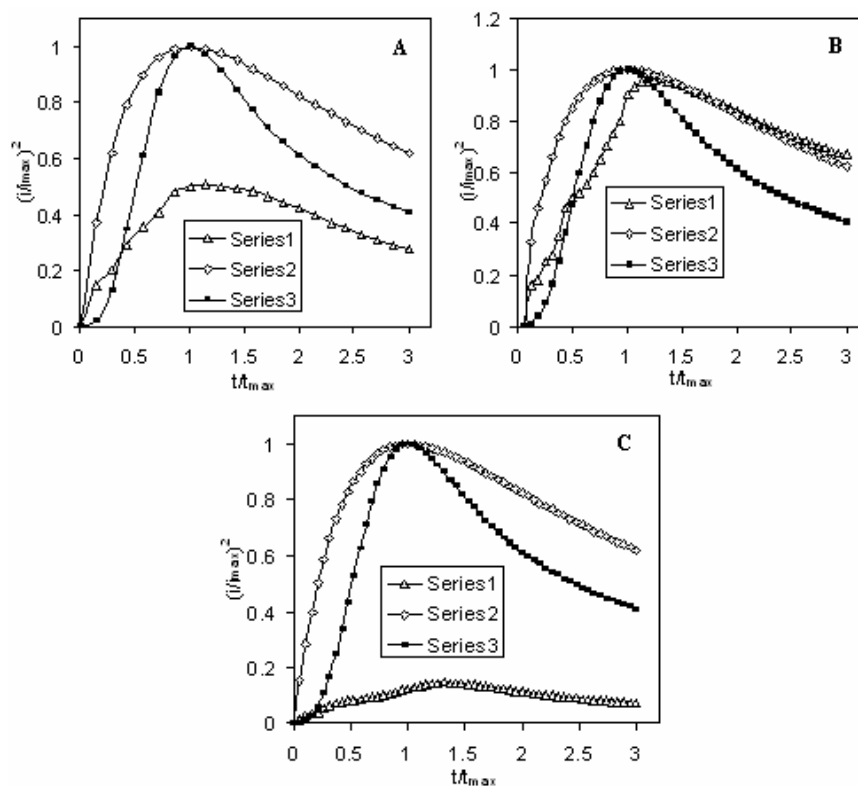


Figure 7. The fitting of experimental curves with theoretical curves (Series 1: Experimental curve, Series 2: Instantaneous curve and Series 3: Progressive curve)

The dependence of instantaneous and progressive nuclei density on the various complexing agents is shown in the figure 8. The plot reveals that the nuclei density N_0 and N_{sat} are strongly dependent on complexing agents. For the bath in absence of complexing agent (sample A) may lead to

higher nuclei density, while for the samples deposited using EDTA and citric acid have lower values of N_0 and N_{sat} . Similar reports were reported in presence of additives [15]. This suggests that the complexing agent induces a decrease in the number of density of nuclei formed. The possible reason for this behavior could be the possible complexing effect of Zn^{+2} by the EDTA and citric acid leading to the retardation in the electrodeposition kinetics [19]. Figure 9 illustrates the dependence of nucleation rate constant 'A' on the presence and absence of complexing agents. From the results obtained it is possible to conclude that the presence of complexing agent EDTA and citric acid in the solutions decreased the nucleation rate constant. This may be due to adsorption of the complexing agent at the electrode surface which reduces electrode active area.

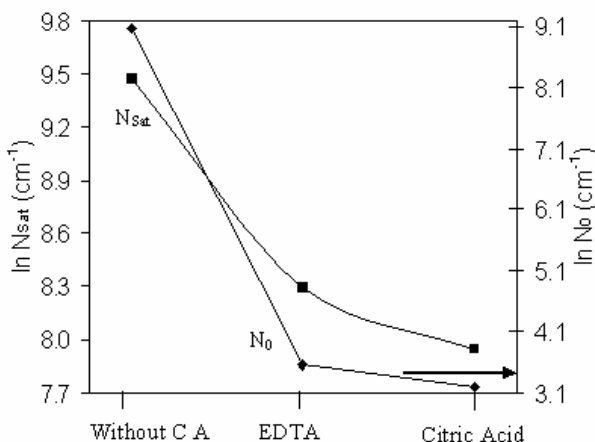


Figure 8. Variation of the number density of formed nuclei (N_0 and N_{sat}) with complexing agents

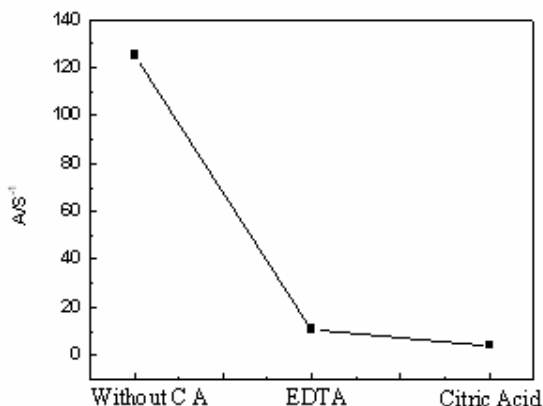


Figure 9. Variation of nucleation rate constant 'A' for progressive nucleation and growth mechanism.

4. CONCLUSIONS

Zinc oxide thin films were electrodeposited onto FTO coated conducting glass substrates by room temperature electrochemical deposition from an aqueous zinc acetate solution. The effect of complexing agents on structural, morphology optical and nucleation and growth mechanism were studied successfully. Different structural and morphological changes were observed for the films

deposited in absence and presence of complexing agents. From the XRD study it is concluded that for the phase pure ZnO film formation addition of complexing agents are needed in view to get desired pH. Flakes like structure and cauliflowers are obtained for the samples deposited without complexing agents. After use of complexing agents the morphology changes to granular and compact structure for EDTA and citric acid respectively. From the Scharifker-Hills model it is concluded that the instantaneous nucleation and growth mechanism prevails for the films deposited in absence and presence of EDTA. But for the samples in presence of citric acid does not follow any type of growth mechanism in studied time domain. From the kinetic parameter study it is confirmed that complexing forms more complexing effect on the Zn^{+2} species. The decreases in N_0 and N_{sat} in presence of EDTA and citric acid may leads to an increase in the critical radius of the nuclei.

ACKNOWLEDGEMENT

The authors wish to acknowledge the U.G.C., New Delhi for the financial support through the DST through FIST (2002-2007) programme and UGC-ASIST (2005-2010) programme.

References

1. S.J. Pearton, D.P. Norton, K. Ip, Y.W. Heo, T. Steiner *Progress in Materials Science* 50 (2005) 293.
2. Lukas Schmidt-Mende and Judith L. MacManus-Driscoll, *Materials Today* 10,5 (2007)40
3. J. Y.Li, G. S.Tompa, S. Liang, C. Gorla, C. Lu, J. Doyle, *J Vac Sci Techol A*, 15 (1997) 1663.
4. Marcus C. Newton and Paul A. Warburton *Materials today*, *Materials Today* 10,5 (2007)50
5. Marcus C Newton, Steven Firth, Takashi Matsuura and Paul A Warburton, *Journal of Physics: Conference Series* 26 (2006) 251.
6. Ying Daia, Yue Zhanga,b, Zhong Lin Wang, *Solid State Communications* 126 (2003) 629.
7. Hongwei Yan, Yingling Yang, Zhengping Fu, Beifang Yang, Linsheng Xia, Shengquan Fu, Fanqing Li, *Electrochemistry Communications* 7 (2005) 1117.
8. G.H. Lee, *Solid State Commun.* 128 (2003) 351.
9. Yingling Yang, Hongwei Yan, Zhengping Fu, Beifang Yang, Linsheng Xia, Yuandong Xu, Jian Zuo, Fanqing Li, *Solid State Communications* 138 (2006) 521.
10. T.W. Kim, K.D. Kwack, H.-K. Kim, Y.S. Yoon, J.H. Bahang, H.L. Park, *Solid State Commun.* 127 (2003) 635.
11. Gao-Ren Li, Ci-Ren Dawa, Qiong Bu, Fu-lin Zhen, Xi-Hong Lu, Zhi-Hai Ke, Hai-En Hong, Chen-Zhong Yao, Peng Liu, Ye-Xiang Tong, *Electrochemistry Communications* 9 (2007) 863.
12. T. Yoshida, K. Terada, D. Schlettwein, T. Oekermann, T. Sugiura, H. Minoura, *Adv. Mater.* 12 (2000) 1214.
13. H. Wang, C. Xie, *J. Crystal Growth*, 291 (2006) 187.
14. J. I. Pankove, *Optical processes in semiconductors*. Dover, New York 1971.
15. R. K. Pandey, S. N. Sahu, S. Chandra, *Handbook of Semiconductor Electrodeposition*, Marcel Dekker Inc., 270 Madison Avenue, New York-10016, (1996).
16. S. B. Sadale and P. S. Patil, *Solid State Ionics*, 167 (2004) 273.
17. A. Chatterjee, J. Foord, *Diamond and Related Materials*, 15 (2006) 664.
18. G. Trejo, H. Ruiz, R. Ortega Borges and Y. Meas, *J. Appl. Electrochem.* 31 (2001) 685.
19. A. E. Alvarez, D. R. Salinas, *J. Electroanal. Chem.* 566 (2004) 393.
20. A. I. Inamdar, S. H. Mujawar, S. B. Sadale, A. C. sonavane, M. B. Shelar, P. S. Shinde and P. S. Patil, *Solar Energy Matar. Solar Cells*, 91 (2007) 864.B.

21. B. Scharifker and G. Hill, *Electrochim. Acta.* 28 (1983) 879.
22. M. P. Pardave, M. T. Ramirez, I. Gonzalez, A. Serruya and B. Scharifker, *J. Electrochem. Soc.* 143 (5) (1996) 1551.
23. H. H. Wu, S. K. Xu, and S. M. Zhou, *Acta Phys. Chem. Sin.* 1(4) 357 (1985).
24. J. Yu, Y. Chen, H. Yang and Q. Huang *J. Electrochem. Soc.* 146 (5) (1999) 1789.